TECHNICAL DEVELOPMENTS FOR AN ANTIPROTON COLLECTOR AT CERN

B. Autin
CERN, CH-1211 Geneva 23, Switzerland

Introduction

The Antiproton Accumulator (AA) has been designed in 1977 as an element of the experiment for the search of the intermediate bosons W± and Z in the Super Proton Synchrotron used in the collider mode. In spite of the limited luminosity obtained during the first physics runs in 1981 it was anticipated that the machine would be good enough to reach its objective. This optimism was confirmed by the discovery of the famous bosons this year and even turned into the enthusiasm of meeting new challenges using the W as a particle factory. This venture requires luminosities at least equal to 10^{30} cm^{-2} s^{-1} and therefore an upgraded source of antiprotons. In 1982, basic studies on antiproton collection and stochastic cooling have been performed and the concept of an Antiproton Collector (AC) has emerged[1]. This machine would be a ring of large acceptance located upstream to the present accumulator, capable of collecting 10^8 antiprotons every 2.4 s. Moreover, it was realized that as high a flux would be extremely useful for low energy antiproton physics in LEAR.

The basic characteristics of the AC are transverse acceptances of 200π mm.mrad, and a momentum acceptance of 6%. In order to satisfy the conditions imposed by the stochastic accumulation in the present upgraded accumulator the transverse beam emittances must be lowered to 5π mm.mrad and the relative momentum spread to $2^0/_{00}$.

Technical breakthroughs have to be made in two fields essentially:

- the focusing of large angles associated with large emittances.
- the extension of stochastic cooling systems in the gigahertz range with a broad pass-band and a high power.

Target and High Field Gradient Lenses

The CERN proton synchrotron produces more than 10^9 antiprotons each time the proton beam impinges the target. To capture less than 10% of the total production seems to be in reach. 10^8 antiprotons represents a factor 16 over the usual number of antiprotons injected at each pulse into the AA. With some simplifications, the factor 16 can be decomposed into three factors.

- a factor 4 due to a quadruple momentum acceptance;
- a factor 2 due to a double transverse acceptance;
- a factor 2 due to the compression of the phase space created by a strong magnetic field around the target.

Pulsed target

The principle of a pulsed target is illustrated in Fig. 1 in the ideal case of an infinitely thin target. In absence of magnetic field, the production diagram in the phase space (x,x') at the end of the target has the well-known shape of a "butterfly". If the target is imbedded in a medium which carries a current of density j which flows parallel to the target, the antiprotons of charge e and momentum p emitted in a radial plane are submitted to an integrated focusing strength:

$$\sqrt{K}\,\ell = \frac{e}{p} \cdot \frac{\mu_0 j}{2}\,\ell ,$$

where $\mu_0 = 4\pi \cdot 10^{-7}$ and ℓ is the length of trajectory in the magnetic field. When $\sqrt{K}\,\ell$ is equal to π, the

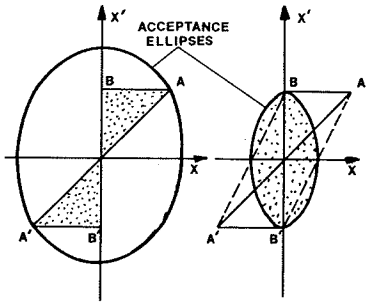

a) without field b) with linear field

Figure 1 - Principle of phase space compression.

segments OA and OA' are mapped onto OB' and OB, and segments BA and B'A' are mapped onto the half-ellipses $\overline{BB'}$ and $\overline{B'B}$. Such a diagram is clearly better matched than a "butterfly" to the elliptical acceptances of a magnetic transfer channel composed of quadrupoles. In practice, the motion of the skew particles is more complicated, the target has a finite thickness and the magnetic field may obey various laws: linear inside a conductor, hyperbolic outside it, combination of linear and hyperbolic laws in a hollow conductor, etc. In order to cope with practical configurations, a general program incorporating detailed Monte Carlo computations has been coded. A typical comparison between two types of structures is given in Table 1.

Table 1

Structure	p-emittance* π (mm.mrad)	p̄-emittance* π (mm.mrad)	Target diameter (mm)	Graphite diameter (mm)	Current copper (kA)	Current graphite (kA)	Gain	Comments
1	1.5 × 1.7	2.5 × 80	3	5	250	-	3.6	p defocusing uncompensated
2	1.5 × 1.7	2.5 × 80	3	5	250	-	4.4	p defocusing uncompensated
3	1 × 2.5	3.6 × 56	2	5	-	250	3.6	pure graphite
4	1 × 2.5	3.6 × 56	2	5	-	250	3.3	on doped graphite

The best efficiency is obtained with structure 2 at the cost of extra proton and antiproton focusing. The final choice will be based on both efficiency and reliability of the target under operational conditions. Fig. 2 gives an example of target structure which is being fabricated.

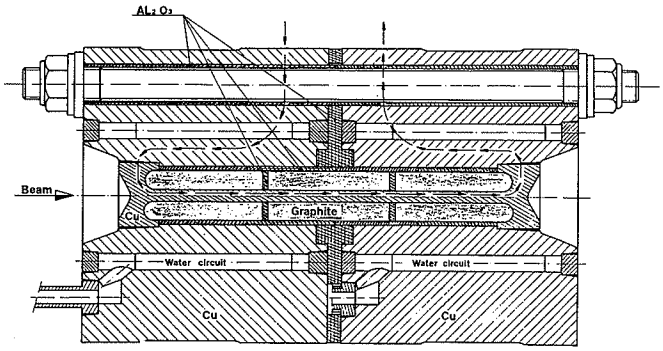

Figure 2 - Current Carrying Target.

Strong Focusing Lenses

Particles of 3.5 GeV/c momentum emitted at as large angles as 80 mrad cannot be focused by conventional quadrupoles. The required high field gradient can only be obtained with high density currents. The current carrying medium must re-absorb the antiprotons as little as possible.

From this only viewpoint a plasma lens is the best choice and a collaboration is on the way with the universities of Erlangen and Naples. An experimental set-up already exists (Fig. 3) and the characteristics of the first discharges are presented in Fig. 4. Eventually the current must reach a value of the order of 500 kA. Present efforts are oriented towards the reduction of the internal resistance, the design of a pulse former network and the observation of the development of the pinch using a streak camera. The difficult problem in operating a plasma lens relies in the stability and the reproducibility of the discharge.

An alternative solution consists of using lithium as a conductor and two types of lenses are prepared in collaboration with Karlsruhe Kernforschung Zenter. Their characteristics are summarized in Table 2.

A water cooled lithium lens is drawn in Fig. 5. Pressure and fatigue tests will be made with a pulsed hydraulic system (6000 bars) whereas filling parameters for the lithium are predetermined with indium which has plastic properties similar to those of lithium.

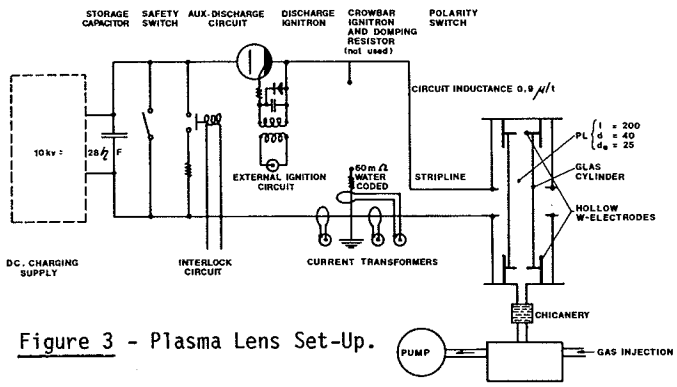

Figure 3 - Plasma Lens Set-Up.

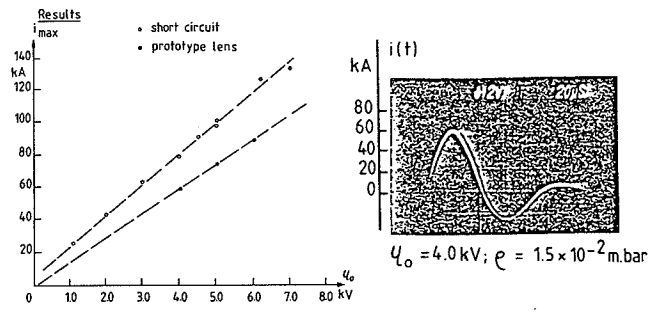

Figure 4 - Characteristics of a Plasma Discharge.

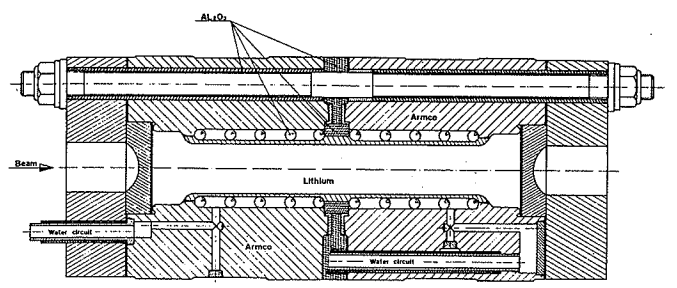

Figure 5 - Lithium Lens Structure.

Table 2 - Lithium lens characteristics

	Model No. 1	Model No.2
Diameter (cm)	2	4
Length (cm)	10	10
Current (kA)	500	850
Resistance (μΩ)	56	16
Pulse length (cm)	1	4
Maximum field (T)	10	8.5
Deposited energy per pulse (kJ)	7	20
Average power (kW)	2.9	8.3
Temperature (°C)	124	89
Thickness of the stainless steel container wall for a 5% current bypass (mm)	1.1	2.2

Stochastic Cooling Systems

Once the beam is focused to the input of the magnetic transfer channel it is transported and injected into the AC ring (Fig. 6) where it is submitted to three treatments before ejection towards the AA ring.

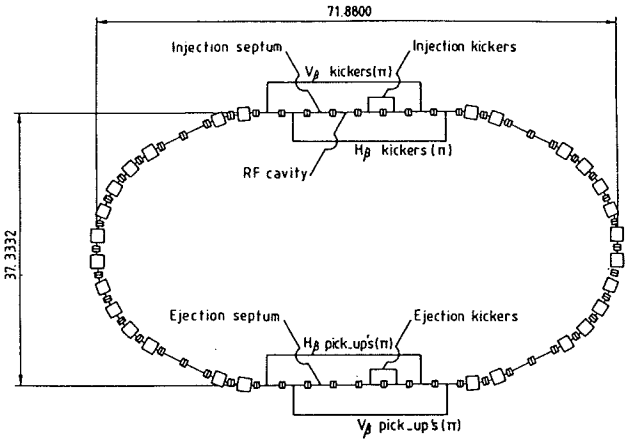

Figure 6 - Example of System Integration in a Lattice.

i. Debunching of the short pulses (14 ns) in the very first turns. Using a sequence of bunch rotation technique and adiabatic turn-off that we shall not describe in detail, the relative beam momentum spread drops from 6% to 1.5%.

ii. In the following second, the transverse beam emittance is stochastically cooled from 200π mm.mrad down to 5π mm.mrad.

iii. In the last second, it is the momentum spread which is stochastically cooled to $2\,^0/_{00}$ using the filter technique.

In practice, a certain overlap will occur between the two types of cooling. Both coolings are fast, require a broadband (2 GHz) and a high electronic power (several kW). As they are power limited, the power is used optimally during all the process by varying the gain of the system. In the case of the betatron cooling, the gain variation is obtained by fitting dynamically the pick-up and kicker electrode gap to the beam size, whereas it is the transfer impedance of the filter which is adjusted for the momentum cooling. The coherent effect dominates the cooling during the greatest part of the process; the diffusion related to the thermal noise is minimized by operating pick-up terminating resistors and low noise preamplifiers at low temperature (40°K). Broadband and low noise amplifiers are being

developed for radioastronomy[2] and for stochastic cooling[3]. On the power side, traveling wave tubes[4] delivering several kilowatts between 4 and 8 GHz exist, they make use of the brazed helix technology; with the reserve of a good phase linearity, the construction of these tubes can be readily transposed into the 2-4 GHz range. However, these devices are expensive and the research at CERN has been oriented towards staggered tune systems which are certainly much cheaper and more flexible (L. Thorndahl).

Staggered Tunes Systems

A set of pairs of electrodes is composed of M electrodes tuned at a quarter wavelength ($\lambda/4$) and connected by ($\lambda/2$) delay lines (Fig. 7). M may vary from group to group. Because of these connections, amplifier attached to a given group remains matched to the structure even when the impedance varies during the motion of the electrode (betatron case). It was calculated that when the impedance is halved the spread in phase does not exceed ±10 degrees for $|\Delta f/f_0| < 2\%$.

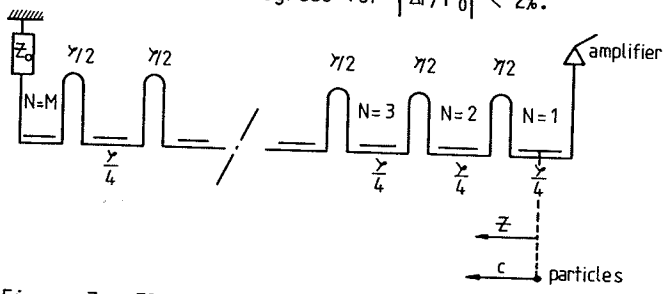

Figure 7 - Electrode Module in a Staggered Tunes System

i. Pick-up's. A sample of particles which grazes the surface of the electrode generates an image current which propagates against the particle displacement:

$$I = I_0 e^{j\omega(t-z/c)}.$$

t is the time at which the signal is generated when the particle is located at the position z:

$$z = -ct + (N-1)(\lambda/2).$$

The voltage U coupled onto the N-th electrode is such that:

$$\frac{dU}{dt} = Z_0 \frac{dI}{dt},$$

Z_0 being the electrode impedance. The integrated voltage at the end of M electrodes is:

$$U_M = jI_0Z_0 \frac{\cos(\frac{\pi}{2}\frac{\Delta\omega}{\omega_0}) \cdot \sin(\pi \frac{\Delta\omega}{\omega_0} M)}{\pi \frac{\Delta\omega}{\omega_0}} e^{-j\pi(M-1)(\Delta\omega/\omega_0)}$$

The phase is:

$$\phi = -\pi(M-1)\frac{\Delta\omega}{\omega_0}$$

and the group delay:

$$\frac{d\phi}{d\omega} = -\frac{M-1}{2f_0}$$

If the overlap between each group occurs at -6 dB points:

$$\Delta\omega = \pm 0.6 \frac{\omega_0}{M}$$

In the AC case, M varies from 5 to 14 between 1 and 3 GHz for a constant 250 MHz bandwidth of the GaAsFET amplifier. The signals produced at the end of each group are amplified and combined on a common board.

ii. Kickers. The kicker structure is reciprocal to the pick-up structure. The voltage wave is $(U_0/2)e^{j\omega(t-z/c)}$ At the N-th gaps, the voltage is:

$$U = U_0 e^{-2\pi jN(\Delta f/f_0)}$$

and the total voltage applied to the particle at the end of a group of M electrodes is:

$$U_M = U_0 \frac{\sin(\pi M \Delta f/f_0)}{\pi \Delta f/f_0} e^{-j\pi M(\Delta f/f_0)}$$

The analysis made for the pick-up's can be repeated for the kickers. The practical difference is in the nature of the amplifier which is a microwave triode with a 25 MHz bandwidth at 3 dB.

Electronic Notch Filter

The calculations of the momentum cooling have been made assuming that the filter was a superconducting coaxial line connected in parallel with a variable resistor. Another type of "notch" filter is being investigated (F. Pedersen). The bandwidth is divided into subbands which are transposed at low frequency using local oscillators and mixers (Fig. 8). Each subband contains a certain number of harmonics of the revolution frequency which are generated by a synthesizer. The beating of the harmonic frequency with the signal gives a

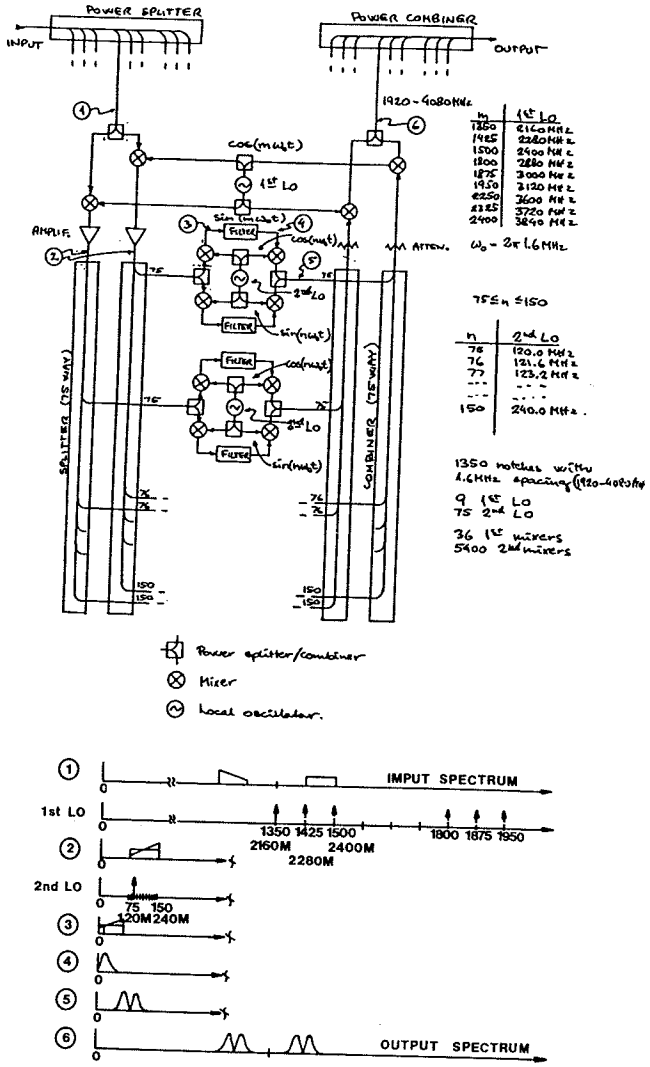

Figure 8 - Electronic Notch Filter.

new signal near the zero frequency, this signal is filtered and reconverted to high frequency. The combination of the cosine and sine channels reproduces the "notch"pattern. Systems based upon this principle have already been used but not to such an extent. The mass production of mixers and local oscillators has to be carefully evaluated. The potential advantage of this technique lies in the shaping of the filter response to match an optimal gain law for the momentum cooling.

Influence of the wave guide modes

There is an apparent dilemna in working at high frequencies with large emittance beams because microwave modes having a wavelength shorter than the cut-off wavelength of the vacuum chamber can propagate and seriously alter the response of the various systems. In fact, this problem is not new and has been successfully solved for the high frequency systems of the AA ring and the experience gained so far will be applied to the AC ring. Moreover, the wave guide modes do not propagate at the same velocity as the TEM mode and their cumulative effect over a great number of electrodes cancels up to a certain point (Fig. 9). However, this problem has to be studied with a great care and a special model of pick-up's has been installed in the SPS and will be tested soon (Fig. 10).

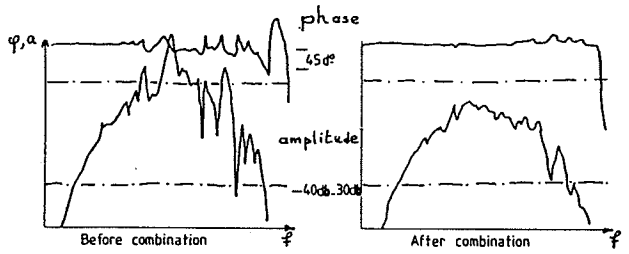

Figure 9 - Effect of Microwave modes on the Pick-Up Response.

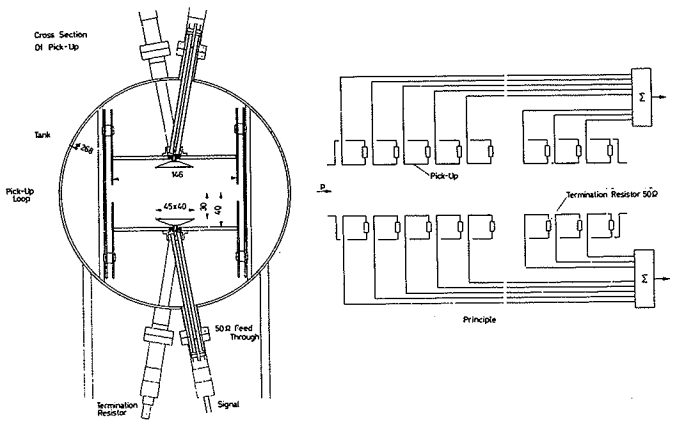

Figure 10 - Experimental Cooling Pick-up Installed in the SPS. 16 loop pairs, spaced by 4.8 cm, are used to obtain both intensity modulation signals (sum of all loop signals) as well as vertical position signals (difference between upper and lower sums). Between the loops and the adding networks fixed delays are inserted such that signals induced by one particle in the 16 loops arrive simultaneously in the 2 adding networks (constructive interference). The structure works from 1 to 2 GHz, i.e. above the TE mode cut off at 1 GHz. With many loops TE mode signals are expected to average out due to $V_{ph} > C$.

Conclusion

The interest and the principles of an antiproton collector added to the antiproton accumulator are firmly established. For most of the special components the design stage is well advanced. In the case of the stochastic cooling systems, the principles of the staggered tunes and of the electronic notch filters seem to be very promising. Experimental set-ups already exist for testing the pick-up response with a real beam, for a plasma lens and for technological developments of the lithium lens. Operational tests of a pulsed target and of the Fermilab lithium lens are foreseen in a very near future to improve the antiproton yield in the accumulator. In brief, we are still far from the end of the race but our heart has a good pace.

References

1. B. Autin, The Future of the Antiproton Accumulator, Proc. of the 18th Rencontres de Moriond (March 1983).

2. S. Weinreb, D. Fenstermacher, R. Harris, IEEE Trans. on Microwave Theory and Techniques, Vol. MTT-30, No 6, p 849 (June 1982).

3. B. Leskovar and C.C. Lo, Proc. of the 1983 Particle Acc. Conf., Santa Fe (March 1983).

4. Tube à Onde Progressive TH 3640, Thomson-CSF Technical Note TEH 4941.

Acknowledgements

This paper is a review of the work made by two study groups:

i. Target and Lenses composed of: B. Autin, R. Bellone, K. Frank, C.D. Johnson, E. Jones, B. Pincott, H. Riege, J.C. Schnuriger, R. Seeböck, T.R. Sherwood, P. Sievers, H.-H. Umstätter, S. van der Meer

ii. High Frequency Systems composed of: B. Autin, G. Carron, R. Garoby, K. Hollingworth, E. Jones, S. Milner, F. Pedersen, C. Taylor, L. Thorndahl, H.-H. Umstätter, S. van der Meer.

It is also a pleasure to thank the members of the Tevatron I project at Fermilab for their precious help and excellent spirit in the exchange of ideas and know how.